NATURAL SCIENCE REVIEW **3** 200803 (2026)
nsr.jinr.int

Methodology, applications, and results of dielectric track detectors in heavy nuclei identification

S. A. Gorbunov[1], N. S. Konovalova[1], N. M. Okateva*[1], N. G. Polukhina[1], T. V. Shchedrina[1], N. I. Starkov[1], E. N. Starkova[1], and A. E. Volkov[1]

[1] *Lebedev Physical Institute of the Russian Academy of Sciences, 119991, Moscow, Russia*

Abstract

The results of the research partnership between the Flerov Laboratory of Nuclear Reactions of the Joint Institute for Nuclear Research (FLNR JINR) and the Laboratory of Fundamental Particles of the Lebedev Physical Institute (LFP LPI) are presented. The publication focuses on two areas: the search for tracks of superheavy nuclei in pallasite meteorites (OLIMPIYA experiment) and testing of various dielectric materials (glasses and micas) as detectors of heavy charged particles.

Keywords: superheavy nuclei, image recognition, identification, dielectric detectors, meteorite olivine

DOI: 10.54546/NaturalSciRev.200803

1. Introduction

The existence in nature, laboratory synthesis, and study of the properties of elements with atomic numbers greater than 100 are of fundamental interest to nuclear physics. The lifetime of these elements, which are currently synthesized only artificially, decreases dramatically with increasing atomic number. On the other hand, the Nuclear Shell Model [1] points to a possible significant increase in the lifetime for nuclei with completed shells, which form the "Islands of Stability" [2, 3]. The theory predicts that closed shells formed by the "magic" numbers of protons (114–126) and neutrons (184 and around), which correspond to the highest binding energy, significantly increase the height of the nuclear fission barrier. The half-lives of some heavy isotopes with a nucleon number close to the "magic" numbers are expected to reach up to millions of years [4].

Scenarios of superheavy element formation are critical for both astrophysics and nuclear theory. Investigating the properties and decay channels of exotic nuclei beyond the stability line not only refines models of element generation and abundance in the Universe but also provides essential data for validating current nuclear physics frameworks.

Progress toward the region of transfermium nuclei was enabled by the development of heavy-ion accelerators, which facilitated the formation of high-Z elements via complete fusion reactions. Consequently, 26 new elements beyond fermium ($Z > 100$) and hundreds of isotopes have

*Corresponding author e-mail address: okatevanm@lebedev.ru

Received: 30 June 2026; Revised: 5 August 2026; Accepted: 9 August 2026; Published: 20 August 2026

been synthesized across the world's leading laboratories [4]: the Flerov Laboratory of Nuclear Reactions at the Joint Institute for Nuclear Research (Russia), the Lawrence Berkeley National Laboratory (USA), the GSI Helmholtz Centre for Heavy Ion Research (Germany), the RIKEN Nishina Center for Accelerator-Based Science (Japan), and some others.

In accelerator-based experiments at JINR, the longest-lived known nuclide $^{289}114$ was synthesized (proton number $Z = 114$, neutron number $N = 175$) [5], with a half-life of 1.9 s, which significantly exceeds those of neighboring isotopes, thereby experimentally validating the predicted existence of long-lived superheavy elements. Currently, leading laboratories (e.g., [6]) are preparing experiments to synthesize the first two elements of the eighth period of the Periodic Table $Z = 119$ and 120, which could provide critical insights into the "Island of Stability" phenomenon.

In parallel, the search for superheavy elements in nature is being performed using stony-iron meteorites (olivine-bearing pallasites), where tracks left by the superheavy nuclei of Galactic Cosmic Rays (GCR) can be preserved and observed within translucent olivine crystals.

In experiments targeting superheavy element synthesis, unambiguous event detection is of paramount importance. Modern detection systems not only record the passage of a heavy particle but also enable its reliable identification. The separation of reaction products by atomic number is achieved using electronic spectrometer systems, solid-state nuclear track detectors (SSNTDs) of various materials, and methods based on differences in the chemical properties of the elements under study. Within solid-state detectors, elemental identification relies on the measurement and analysis of the parameters of tracks, which are formed by the structural and chemical disruption of the detector matrix due to ionization caused by a projectile.

2. Search and study of heavy and superheavy cosmic nuclei tracks in meteoritic olivine

Considering the problem of origin and search for superheavy and exotic nuclei to be one of the key challenges in modern physics [7], Academician V. Ginzburg initiated a search for cosmic-ray relic tracks in meteorite olivine crystals. This concept was realized through the OLIMPIYA (Olivines from Meteorites — Search for Heavy and Superheavy Nuclei) experiment [8], as a collaborative effort between the Laboratory of Fundamental Particles of LPI RAS, the Flerov Laboratory of Nuclear Reactions of JINR, and the Vernadsky Institute of Geochemistry and Analytical Chemistry of RAS.

Nuclei with $Z > 80$ are formed mainly through the rapid neutron capture process (r-process), which theoretical models associate with high-energy astrophysical events such as supernova explosions [9]. Additionally, electromagnetic spectra observations of the GW170817 event by the LIGO–Virgo collaboration [10] verified the synthesis of superheavy elements via the r-process in neutron star mergers and neutron star − black hole mergers (both referred as NSMs) [11]. Prolonged exposure to cosmic rays in outer space makes meteorites natural witnesses of rare cosmic events, including NSMs, that drive the r-process. Consequently, meteorites serve as unique detectors for superheavy nuclei fluxes, which have an extremely low abundance in cosmic rays.

Pallasite meteorites consist of an iron-nickel matrix embedded with inclusions of magnesium-iron silicate olivine mineral $(Mg_{0.88}Fe_{0.12})_2SiO_4$. These inclusions represent the translucent, yellowish crystals with linear dimensions of up to 1 cm (Figure 1).

High-energy heavy nuclei decelerating in olivine damage its crystal lattice, forming an extended track with altered structural and chemical properties of the mineral. The rate of etching in special chemical solutions within the damaged crystal area is orders of magnitude higher than

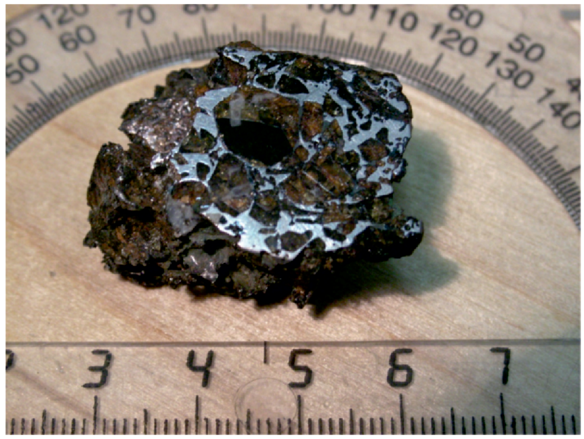

Figure 1. Fragment of the Eagle Station meteorite, one of the two meteorites used in the OLIMPIYA experiment.

the one of the undamaged material. As a result, a hollow channel forms along the trajectory of a heavy charged particle. The size and shape of this channel depend on the degree of damage to the material at the atomic level [12, 13].

The key advantages of using meteorite olivine crystals as natural detectors to register and study superheavy GCR nuclei are listed below.

1. Compared with other SSNTDs, olivine is completely free from the background of tracks of nuclei with $Z < 26$. This is due to a sufficiently high threshold of specific energy loss required to form chemically etchable tracks ($dE/dx \approx 18$ MeV/(mg cm^{-2}) [14]). Consequently, etchable channels in olivine are formed only by nuclei starting from the iron group, enabling the study the heavy and superheavy nuclei tracks under low background conditions.

2. Olivine crystals constitute about 65 vol.% of pallasite meteorites.

3. The olivine crystals examined in this experiment possess several specific characteristics that make them preferable for the track analysis:

— crystal size: large intact crystals allow for the etching and subsequent analysis of tracks up to 1–2 mm in length;

— chemical homogeneity: the crystals share a uniform chemical composition within each individual pallasite meteorite;

— optical transparency: high transparency allows the etched tracks to be clearly observed and documented under an optical microscope at depths reaching several hundred micrometers;

— isotropic response: the length of the etched tracks and the etching rate are independent of their crystallographic orientation relative to the symmetry axes of the olivine crystal [15];

— lattice robustness: the registration efficiency of charged particles is independent of the structural ordering within the olivine crystal lattice [15];

— high track stability: microstructural lattice defects induced along the deceleration paths of charged particles remain exceptionally well-preserved throughout the meteorite's prolonged cosmic-ray exposure in space.

4. The prolonged exposure of the meteorites under study to cosmic rays, spanning up to 200 million years [16], provides sufficient statistics of the registered tracks of superheavy GCR elements, whose flux is 5–6 orders of magnitude lower than that of the iron group nuclei [17]. At a depth of ~ 5 cm from the pre-atmospheric meteorite surface, approximately 10^2–10^3 tracks of nuclei with $Z > 90$ are formed per 1 cm^3 of olivine over 10^8 years, while up to 10^4 such tracks accumulate at depths of less than ~ 1 cm. In our case, the olivine crystals examined in

the OLIMPIYA experiment were located at pre-atmospheric depths of 1.5–4 cm for the Eagle Station meteorite and 4–8 cm for the Marjalahti meteorite [18].

The first tracks of iron-group nuclei in meteorites were discovered in 1964 [19]. From the 1970s until 2003, FLNR JINR carried out searches for superheavy cosmic-ray nuclei tracks within olivine crystals from the Marjalahti and Eagle Station pallasites [20, 21]. The development of the high-tech PAVICOM automated scanning complex at LPI in the early 2000s [22] enabled the systematic study of these pallasite fragments.

One of the parameters measured after chemical etching was the track length L, which corresponded to the damaged region where the etching rate along the projectile's path was high enough to be detected [23]. The total length of the etched track is functionally connected with the charge of the decelerating nucleus. In the OLIMPIYA experiment, for estimating the nucleus charge, the etching rate along the track (V_{TR}) was used as a second key characteristic. This rate depends significantly on the particle charge.

The technique of sequential, stepwise cutting and etching of crystal surface layers was employed to ensure the accurate determination of track parameters and maximize the effective volume of the investigated crystal. Upon completion of the initial measurement stage on the etched crystal, a surface layer with a thickness of 50–60 μm was removed via precision grinding. Subsequently, the etching and measurement procedure was repeated on the newly exposed layer. The newly detected track fragments were then reconstructed and aligned with the corresponding segments previously recorded in the removed layers. The track etching rates were determined at each processing stage. Comparing the etching rates measured across successive layers ensured high-accuracy determination of the track parameters required for nuclear charge identification. Calibration experiments conducted on accelerators, followed by subsequent data analysis, established a correlation between the measured track length L, the track etching rate V_{TR}, and the projectile charge $Z(L, V_{TR})$ for nuclei within the charge range of 50 (Sn) to 92 (U) and at energies spanning 50–400 MeV/nucleon [24]. The derived function $Z(L, V_{TR})$ was subsequently extrapolated to the region of transuranic elements (see Figure 2) and applied in the OLIMPIYA experiment to identify the charges of nuclei that produced the etched tracks.

In addition, a microscopic multiscale model was developed to describe nuclei deceleration in olivine, structure and chemical changes around nucleus trajectory and track etching rate. This approach combines (1) Monte-Carlo code TREKIS [25] describing excitation and relaxation of the electronic system of a target and energy transfer to target atoms, molecular dynamics

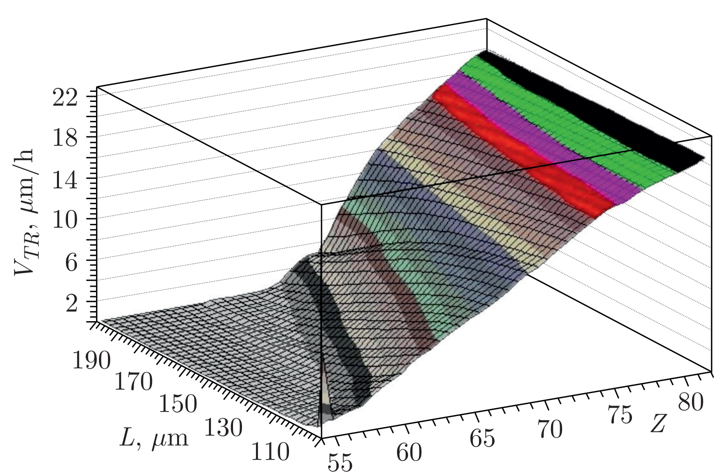

Figure 2. Three-dimensional functional surface $Z(L, V_{TR})$ connecting the measured length of etched tracks L, the track etching rate V_{TR}, and the charge Z of nuclei.

simulation of the excitation and structure changes in the atomic system of olivine; (2) molecular dynamics calculation of the chemical reaction rate increase along and around the nucleus trajectory based on the transition state theory; and (3) wet chemical etching simulation, which takes into account diffusion-controlled etching in the nanometric vicinity of the nucleus trajectory, reaction-controlled etching in the track halo, and gradual transition between these two regimes [13]. The results of simulations are presented in Figure 3.

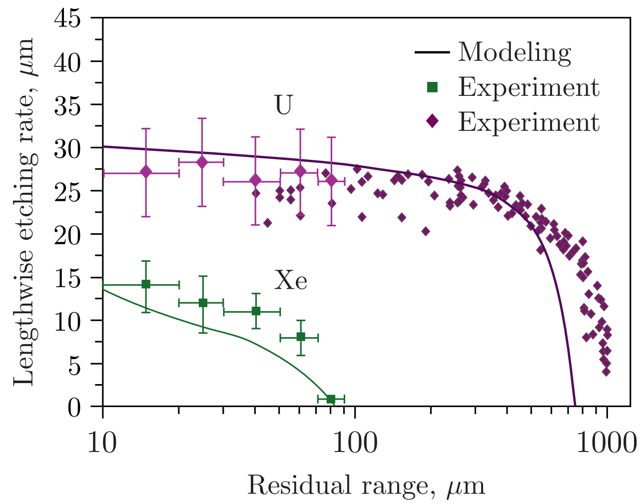

Figure 3. The track etching rates as functions of the residual ranges of 1.7-GeV Xe and 16-GeV U ions in olivine $(Mg_{0.11}Fe_{0.89})_2SiO_4$. Solid lines present the etching rate obtained from the modeling. Experimental values are indicated by squares and rhombuses with error bars. Registration threshold of visibility 400 nm is assumed.

In the experiment, 890 crystals of meteoritic olivine were processed, which provided the statistics of 21 743 processed tracks of heavy GCR nuclei with $Z > 55$. The charge spectrum in Figure 4 presents the relative abundance of heavy nuclei with $Z \geqslant 55$ obtained in two meteorites. The uncertainty of determining the charge does not exceed $\Delta Z = 2$ with a confidence interval of 70%.

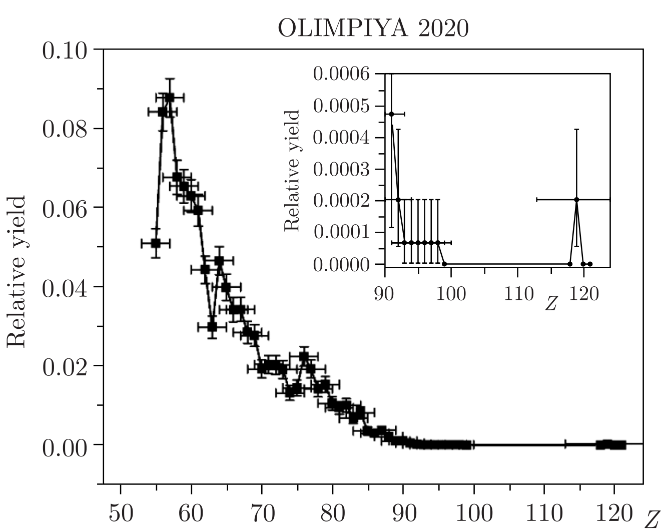

Figure 4. Relative yield of GCR nuclei registered with 70% confidence interval in two meteorites processed in the OLIMPIYA experiment.

An analysis of the differences in the distributions of superheavy nuclei recorded in olivine crystals from Marjalahti and Eagle Station pallasites of different cosmic-ray exposure (CRE) ages, 35–71 and 178–205 Myr, respectively, where Myr is “million years” [26], was carried out. The difference in the distributions exceeds the acceptance error and is clearly distinguishable in Figure 5. The data obtained made it possible to analyze the changes in the GCR flux over the past 200 Myr. In addition to the difference between the meteorites themselves, the comparison

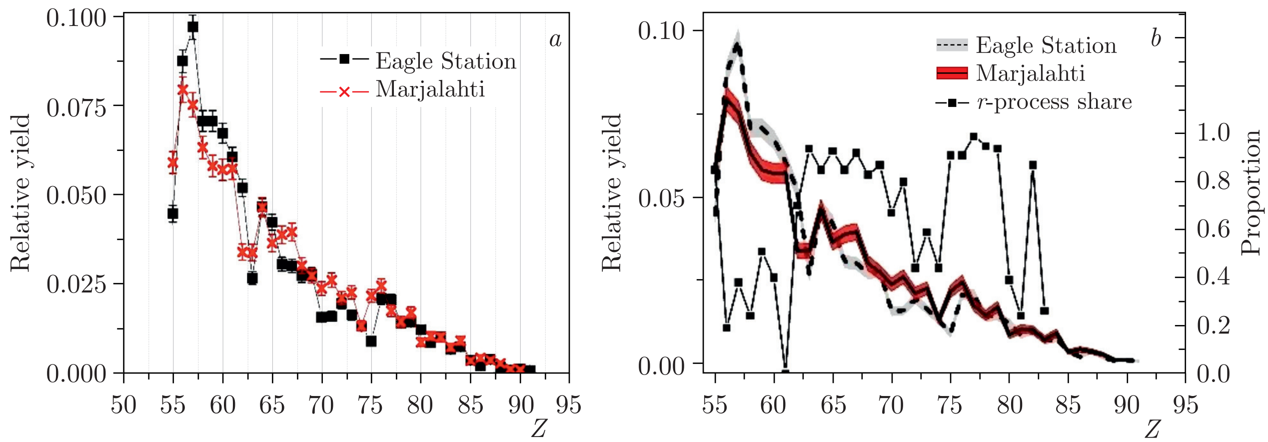

Figure 5. Comparison of the charge spectra of GCR nuclei obtained in two pallasite meteorites with different CRE ages (a) and superimposing this comparison on the contribution of r-processes in the element synthesis [27] (b).

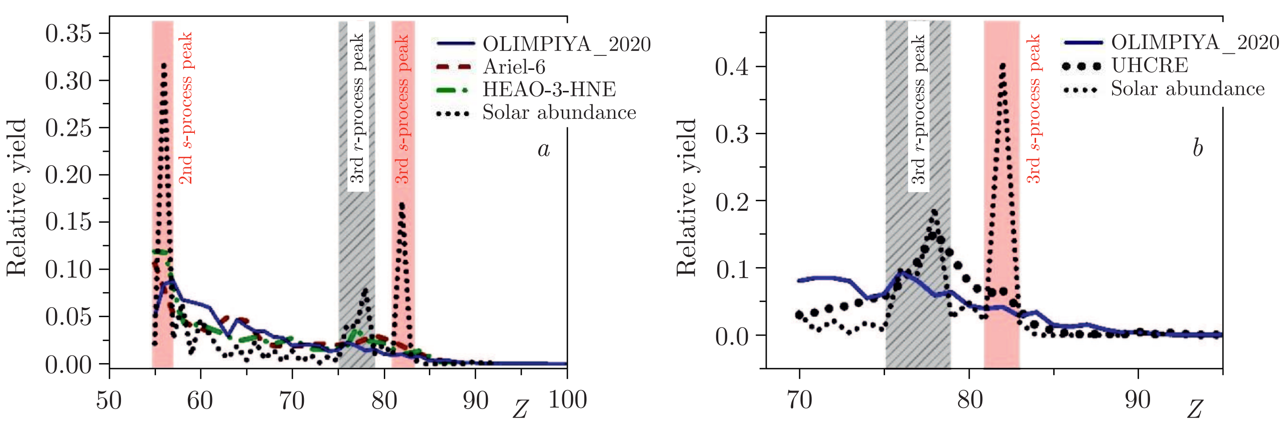

Figure 6. Relative abundances of nuclei registered in the OLIMPIYA experiment in comparison with the distributions from the satellite experiments and with the Solar abundances [27, 28]. Normalization is made for $Z \geqslant 55$ (a) and $Z \geqslant 70$ (b).

revealed significant discrepancies in the content of nuclei detected in meteorites and in satellite detectors (Figure 6).

The nature of the observed differences indicates at least two rare events of cosmic nucleosynthesis events with an increased yield of r-elements, which influenced the GCR fluxes in the vicinity of the Solar System during the period under review. The interpretation of the results is based on a comparison of the contribution of astrophysical sources of two types: events related to nucleosynthesis in asymptotic giant stars with subsequent acceleration of elements during supernova explosions (AGB&SN channel), and fusion events of neutron stars or neutron stars with black holes (NSM channel). The analysis held shows the rarity of NSM events near the Solar System. However, these events provide a significant share of heavy element supply in the Solar System.

One of the most interesting results of the OLIMPIYA experiment is the registration of three ultra-long tracks of more than 500 μm each with etching rate exceeding 35 μm/h (Figure 7). Once the maximum value of the experimentally measured etching rate for uranium nuclei tracks in olivine is 26 ± 1 μm/h, one can assume that the charges of these nuclei significantly exceed the charge of uranium.

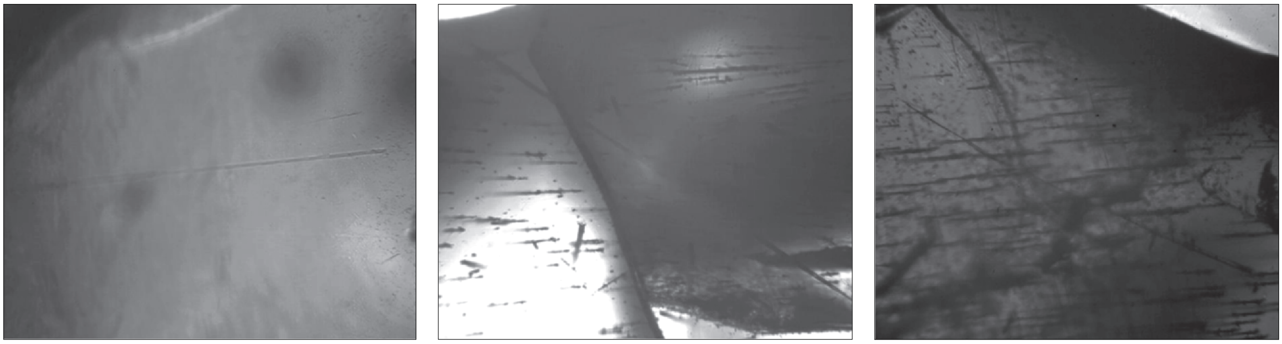

Figure 7. Micrographs of three extra-long etched tracks in meteoritic olivine.

Regression analysis of the track etching rate yielded a charge estimation for these nuclei of 119^{+10}_{-6} at a 95% confidence level. The uncertainties were evaluated according to the method described in [29] using measurement errors obtained in calibration experiments involving fitting the experimental data points with a straight line and constructing a confidence corridor for the specified level.

According to the assessment, the minimum lifetime T of these nuclei falls within the range of $50 < T < 100$ years [30], which is many orders of magnitude longer than the lifetime of transfermium nuclei synthesized in accelerator experiments. Consequently, the data from the OLIMPIYA experiment provide a compelling argument in favor of the existence of the theoretically predicted island of stability for long-lived nuclei of natural origin.

3. Natural and synthetic dielectric materials as heavy ion detectors

At accelerators, superheavy elements are produced via complete fusion reactions between target nuclei and incident projectiles [31]. To this end, the Superheavy Element Factory was built at the Joint Institute for Nuclear Research (JINR) [6, 32]. The chemical properties of the synthesized elements are investigated using thermochromatography [33, 34], where the newly formed species are transported by an inert carrier gas jet into a thermochromatographic column, capturing electrons to become neutral atoms. A temperature gradient is established along the detector array inside the column. The deposition zones of the atoms along this temperature gradient correlate with their chemical properties, and the exact adsorption sites of the synthesized elements are determined by registering their radioactive decay. During the investigation of the chemical properties of element 112, the maximum deposition temperature reached 35 °C [35]. However, other elements may require substantially higher temperatures, up to several hundred degrees Celsius [36], which imposes strict constraints on the detector types and materials utilized in the column.

At elevated temperatures, track annealing can occur within dielectric materials, resulting in the partial or complete erasure of tracks. Since particle identification in SSNTDs is based directly on the geometric parameters of the tracks, thermal annealing can distort the experimental data. Consequently, when selecting a detector material, it is essential to evaluate the effects of thermal exposure, both during and after irradiation, on the registration sensitivity of detectors subjected to chemical etching.

To this end, various dielectric materials are evaluated to determine their capability to retain tracks of charged particles at elevated temperatures. Samples of both synthetic and natural dielectrics, including various types of glass [37, 38], as well as synthetic and natural micas [39], are irradiated with heavy ions across a wide energy range using the JINR cyclotrons. The selection of these materials is dictated by their physical and chemical properties. They must exhibit high chemical and thermal stability, uniformity, mechanical strength, and optical transparency, that remains stable under high-temperature conditions. A primary criterion for material suitability is the thermal stability of the structural radiation damages induced by the passage of charged particles. To study the influence of elevated temperatures on track retention, the dependence of the track projection length on the detector plane as a function of etching time was investigated under various thermal conditions. Two thermal regimes were evaluated: *in situ* heating (the "heated target" configuration) and post-irradiation annealing. In the *in situ* heating method, preheated samples were irradiated and subsequently maintained at the target temperature for a specified duration. In the case of post-irradiation annealing, the effect of the annealing temperature on both the proportion of preserved tracks and the variation of etched track parameters was systematically investigated.

The PAVICOM group has developed an image processing algorithm for tracks in dielectric materials that differ significantly from that in olivine. The microscope focus depth at forty-fold magnification is $\sim 20{-}22$ μm, and in the focused image of the beginning of the track, its end is usually somewhat blurred in the field of view. The created track processing program includes a contrast enhancement procedure in which the blurred end of the track is also included in a single cluster (the track projection image reconstructed via computer processing), meaning the total cluster length completely corresponds to the projection of the etched channel. The cluster size and the angle of incidence of the beam on the sample surface give the full track length. An example of image processing of Bi tracks in mica is shown in Figure 8.

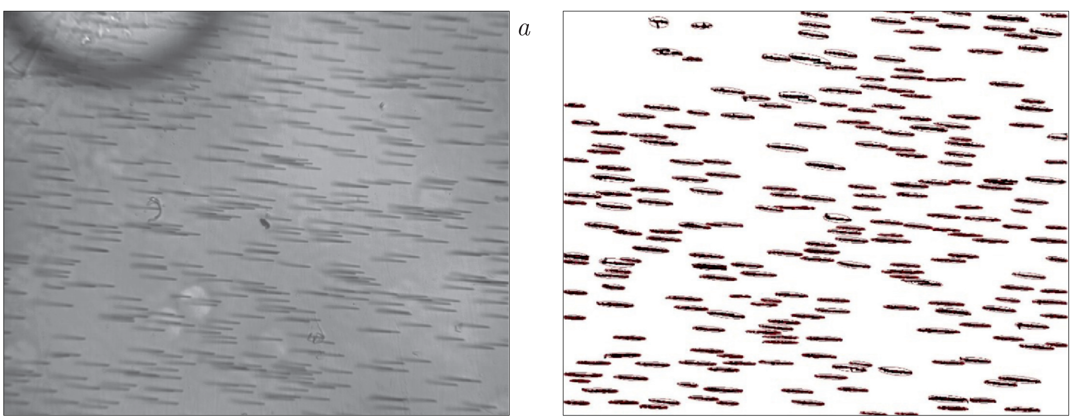

Figure 8. Tracks of accelerated 670-MeV Bi ions in mica (*a*) and the result of their software processing (*b*). The irradiation angle is 45°.

An important part of the research was devoted to the etching mode selection for each material, during which etchant compositions, concentrations, duration of the procedure and temperature regime varied. The etching duration, the stability of the etching solution, and the dynamics of changes in the track geometric parameters demonstrated optimal values when etched in HF hydrofluoric acid at various concentrations.

The etching of the irradiated samples occurs in two stages, which are clearly manifested in the experimental curve representing the track projection length as a function of etching time. A distinct kink is observed on the corresponding graph (Figure 9), with its position matching the particle stopping point within the detector material. The steeper initial section corresponds to the region damaged by the charged particle (the track core) and exhibits a higher etching rate. Beyond the kink, the etching of the undamaged material proceeds at a slower rate. This

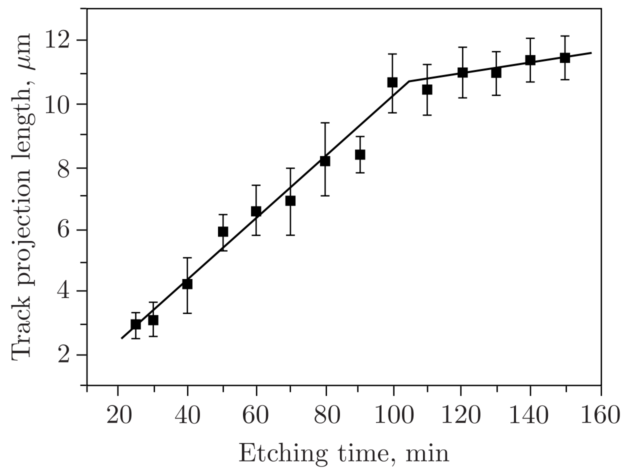

Figure 9. Track projection length of 475-MeV Xe ions in KU-2 quartz glass as a function of etching time.

characteristic variation in the etching rate is utilized to estimate the total particle range within the detector.

The results of these benchmark experiments allow us to classify the studied materials into the following categories based on their track-retention properties:

— glass types in which etched tracks were not detected under an optical microscope (aluminum-calcium AKS-5 and silicate C48-3);

— phosphate glass of SELG brand, where the etched tracks were detected after treatment at room temperature, but no tracks were observed after annealing at 300 °C;

— phosphate glass of the KNFS-3 brand, which retains tracks when heated up to 200 °C, albeit with altered their geometric parameters. No visible tracks appear at higher annealing temperatures. Notably, tracks appear even at "heated target" mode up to 500 °C, though their geometric parameters change;

— quartz glass KU-2, which is capable of preserving ion tracks after post-irradiation heating irradiation up to 500 °C, though accompanied by changes in their geometric parameters;

— glass types in which tracks fail appear after annealing at 300 °C: light (LC-7) crowns, heavy (TK-12) crowns, and leaded glass brands (ZF-6, ZF-501, K-509);

— natural micas ("Indian" muscovite and muscovite with lepidolite [39]), which fully retain track dimensions after annealing at 500 °C;

— artificial mica fluoroflogopite of the SM-310 brand, samples of which were damaged by etching.

The results demonstrate the applicability of natural micas as heavy nuclei detectors at high temperatures. This potential is illustrated with a simulated 3D functional surface relating the charge Z with the measured characteristics of the etched track — the track length L and the etching rate V. This approach is analogous to the method previously employed by the authors in the OLIMPIYA experiment. Modeling with the SRIM program [40] provided the values of the track length L for the Ar, Kr, and Xe nuclei at three energy values in the "Indian" muscovite mica. Figure 10, *a* presents the resulting dependence of the etching rate on the particle charge and energy $V(Z, E)$. For each charge value, the function $V(Z, E)$ was fitted using the parabolic equation $V = A(Z) + B(Z)L + C(Z)L^2$. Consequently, the dependence of coefficients A, B, and C on the charge Z was also approximated by parabolas. Based on this data, an analytical form of the function $V(Z, L)$ was derived (Figure 10, *b*). The similarly constructed dependence of the particle energy on the charge and path $E(Z, L)$ is shown in Figure 10, *c*.

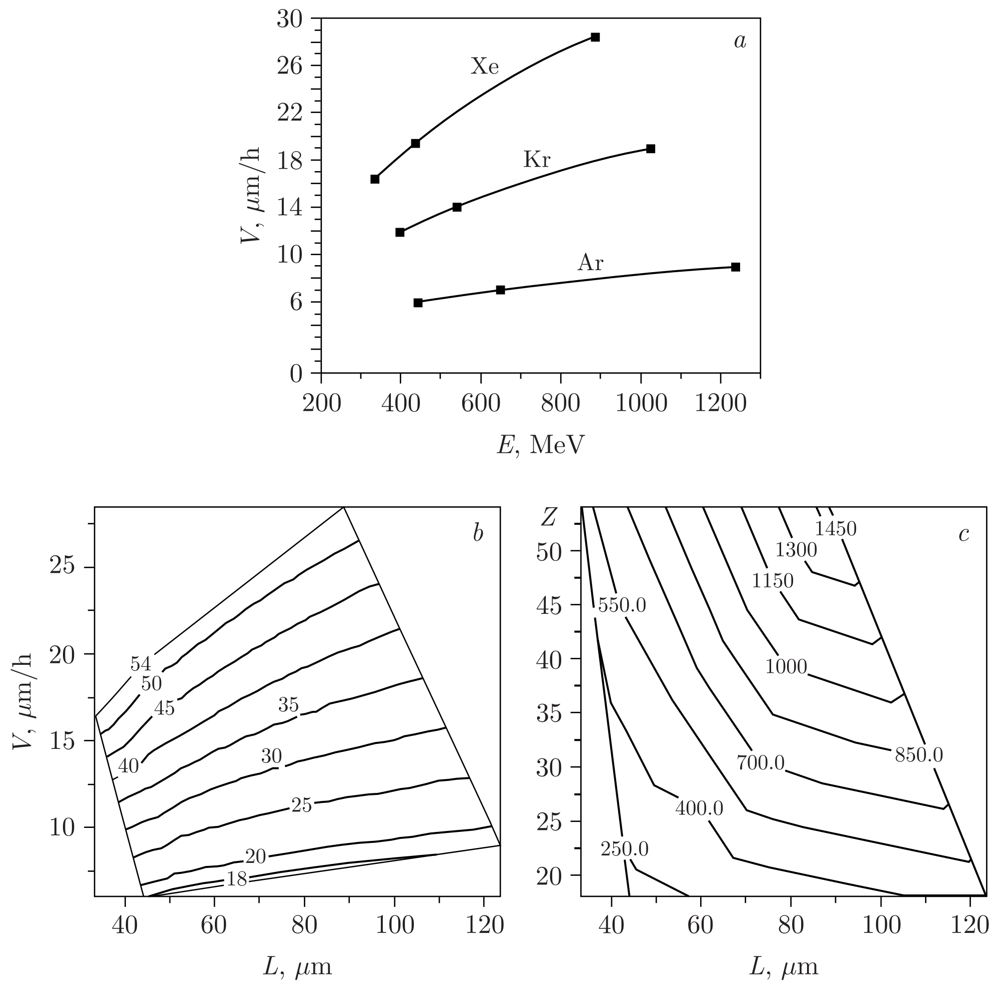

Figure 10. Track etch characteristics for Ar, Kr, and Xe ions in muscovite mica: *a*) etching rate V as a function of ion on charge Z and energy E, fitted using the parabolic equation $V = A(Z) + B(Z)L + C(Z)L^2$; *b*) particle charge $Z(L, V)$ versus the track length L and etching rate V, where numbers on the contour lines indicate the charge values; *c*) particle energy $E(L, Z)$ as a function of track length L and charge Z, with energy values in MeV indicated on the contour lines.

The accuracy of the charge and energy determination method was verified using the SRIM program for the track lengths of iron and barium ions at two energies. First, the etching rate V was calculated using the derived function $V(Z, L)$. Then, the nuclear charge Z and energy E were reconstructed based on the corresponding L and V. The charges and energies determined via the developed algorithm demonstrate good agreement with the reference SRIM data (see Table 1).

Table 1. Comparison of ion charges and energies determined by the SRIM program and with the developed algorithm.

L, mm	V, μm/h	Z		E, MeV	
		SRIM	Algorithm	SRIM	Algorithm
0.038	15.2	46	45.5	500	497
0.057	19.2	46	45.8	800	788
0.052	9.87	26	26.6	375	368
0.082	12.1	26	26.3	550	541

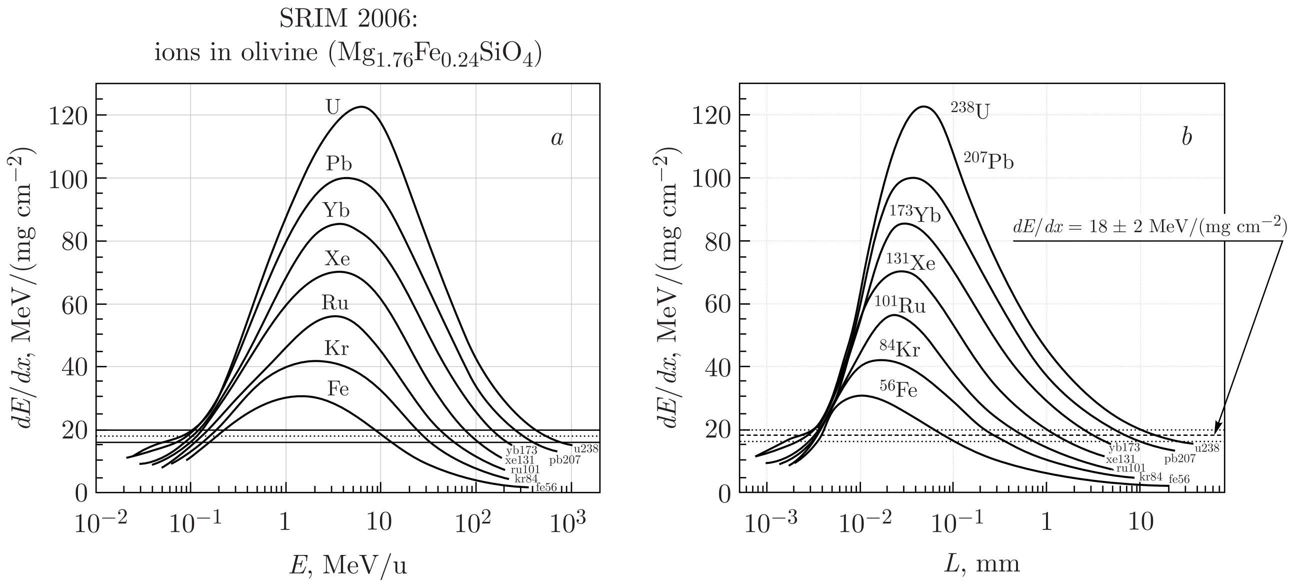

Figure 11. The electronic energy loss of nuclei in olivine as a function of energy E (a) and residual range L (b).

As previously noted, etchable tracks are formed in dielectrics only if the ionization energy loss in the material exceeds a certain threshold value characteristic of that material. Figure 11 displays the ionization loss curves in olivine as a function of the particle energy (Figure 11, a) and the residual range (Figure 11, b), where the threshold value of 18 ± 2 MeV/(mg cm^{-2}) is indicated by horizontal lines. The figure illustrates the maximum energy $E_{\max}$ at which a charged particle can form an etchable track. The corresponding maximum track length $L_{\max}$ is defined as the distance between the two branches of the function at the $E_{\max}$ level (Figure 11, b).

Thus, for iron, the corresponding values make $E_{\max} = 10$ MeV/nucleon and $L_{\max} = 70$ μm, and for uranium, $E_{\max} = 500$ MeV/nucleon and $L_{\max} = 10$ mm.

An interesting result was obtained upon irradiating the "Indian" muscovite samples with argon ions. At all three irradiation energies, 175, 230, and 390 MeV, the measured track length remained unchanged at approximately 30 μm, whereas the SRIM program predicts the total range values of 50, 75, and 130 μm, respectively. This independence of the track length on the initial ion energy suggests that at these selected irradiation energies, the ionization energy loss of Ar ions in mica falls below the track-formation threshold, and 30 μm represents the maximum etchable track length for argon in mica.

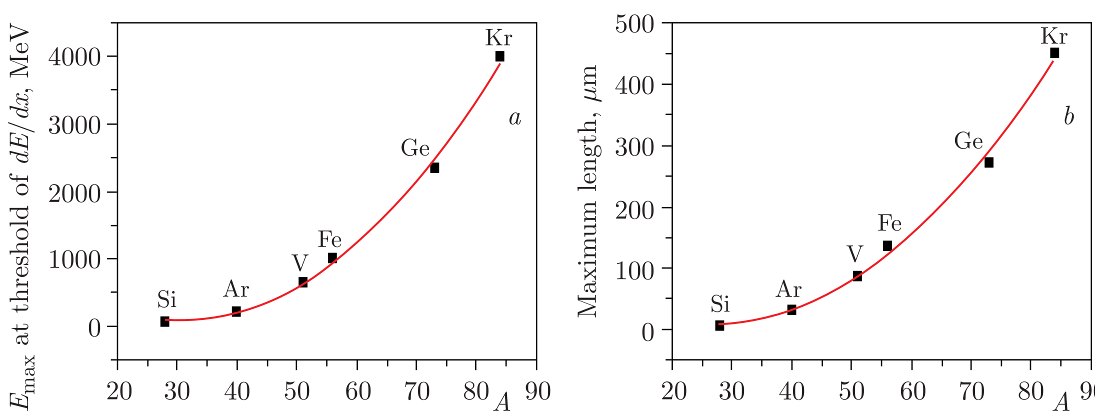

Figure 12. $E_{\max}$ (a) and $L_{\max}$ (b) as a function of mass number A.

The maximum track length $L_{\max}$ of argon ions and their corresponding ionization loss curve in mica allow the track-formation threshold to be determined as $dE/dx = 15.5 \pm 0.5$ MeV/(mg cm^{-2}). The experimentally determined maximum energy $E_{\max}$ for a specific nucleus enables the estimation of $E_{\max}$ and $L_{\max}$ values for other nuclei. Figure 12, *a* shows the dependence of $E_{\max}$ on the mass number A, fitted using a parabolic equation; tracks in mica are formed only by nuclei with energies below this curve. The maximum ionization loss of silicon nuclei is close to the threshold value of $dE/dx = 15$ MeV/(mg cm^{-2}), implying that lighter nuclei do not form etchable tracks in mica. Figure 12, *b* demonstrates the dependence of $L_{\max}$ on A in mica for several nuclei, also approximated by a parabola.

4. Conclusion

JINR and LPI have been collaborating for many years to develop comprehensive physical and engineering solutions for detecting relativistic charged particles across a wide range of experiments. This fruitful collaboration includes experiments utilizing detectors based on the relativistic nuclear emulsion, synthetic and natural dielectric materials, and meteorite olivine.

Efficient processing of track detector data is performed using the advanced PAVICOM optical measuring facility which is widely employed in nuclear, cosmic-ray and high-energy physics. The facility is equipped to provide automated event searching and real-time measurement of particle track parameters across various types of solid-state track.

For two decades, continuous upgrades to the equipment and software of the PAVICOM facility have enabled the processing of large volumes of track detector data. Consequently, the capability to scan large-area emulsion detectors with high spatial resolution offers broad opportunities for addressing both fundamental science, as demonstrated in the OPERA [41] and SND@LHC [42] experiments, and applied problems in the muography of large-scale objects. In muography experiments, analyzing the angular distributions of probing atmospheric muons enables the non-invasive reconstruction of 3D images showing the internal structures of large natural and industrial objects that are otherwise inaccessible to direct observation (see, for example, [43]).

Through the successful long-term partnership between JINR and LPI, a number of major results of modern physics have been achieved. The existing prospects for further collaboration span a wide range of scientific fields, and its potential is far broader than the scope of this article.

Author contributions

S. Gorbunov: Formal analysis, Visualization, Writing — review and editing; N. Konovalova: Investigation, Data curation, Writing — original draft; N. Okateva: Funding acquisition, Resources, Software; N. Polukhina: Conceptualization, Methodology, Supervision, Project administration; T. Shchedrina: Methodology, Investigation; N. Starkov: Conceptualization, Methodology, Formal analysis, Visualization; E. Starkova: Methodology, Investigation, Data curation; A. Volkov: Conceptualization, Validation, Reviewing and Editing.

Conflicts of interest

The authors declare no conflicts of interest.

References

[1] M. Goeppert Mayer, The shell model, Science 145 (1964) 999–1006. https://doi.org/10.1126/science.145.3636.999.

[2] S. G. Nilsson, S. G. Thompson, C. F. Tsang, Stability of superheavy nuclei and their possible occurrence in nature, Phys. Lett. B 28 (1969) 458–461. https://doi.org/10.1016/0370-2693(69)90514-0.

[3] D. J. Dean, Beyond the nuclear shell model, Phys. Today 60 (2007) 48–53. https://doi.org/10.1063/1.2812123.

[4] Yu. Ts. Oganessian, K. Rykaczewski, A beachhead on the island of stability, Phys. Today 68 (2015) 32–38. https://doi.org/10.1063/PT.3.2880.

[5] Yu. Ts. Oganessian et al., Synthesis of superheavy nuclei in the ^{48}Ca + ^{244}Pu reaction: ^{288}114, Phys. Rev. C 62 (2000) 041604. https://doi.org/10.1103/PhysRevC.62.041604.

[6] S. Dmitriev, M. Itkis, Yu. Oganessian, Status and perspectives of the Dubna Superheavy Element Factory, EPJ Web Conf. 131 (2016) 08001. https://doi.org/10.1051/epjconf/201613108001.

[7] V. L. Ginzburg, What problems of physics and astrophysics seem now to be especially important and interesting (thirty years later, already on the verge of XXI century)?, Phys. Usp. 42 (1999) 353–373. https://doi.org/10.1070/PU1999v042n04ABEH000562.

[8] V. L. Ginzburg, E. L. Feinberg, N. G. Polukhina, N. I. Starkov, V. A. Tsarev, Problems and horizons of the search for tracks of heavy and superheavy nuclei in olivine crystals from meteorites (OLIMPIYA project), Doklady Phys. 50 (2005) 283–285. https://doi.org/10.1134/1.1958116.

[9] L. Ahrens, Origin and distribution of the elements: International Series of Monographs in Earth Sciences, 1st Edition, Elsevier, Pergamon, London, 2015.

[10] E. Pian et al., Spectroscopic identification of r-process nucleosynthesis in a double neutron-star merger, Nature 551 (2017) 67–70. https://doi.org/10.1038/nature24298.

[11] D. Kasen, B. Metzger, J. Barnes, E. Quataert, E. Ramirez-Ruiz, Origin of the heavy elements in binary neutron-star mergers from a gravitational wave event, Nature 551 (2017) 80–84. https://doi.org/10.1038/nature24453.

[12] S. A. Gorbunov, A. I. Malakhov, R. A. Rymzhanov, A. E. Volkov, Model of wet chemical etching of swift heavy ions tracks, J. Phys. D: Appl. Phys. 50 (2017) 395306. https://doi.org/10.1088/1361-6463/aa8153.

[13] S. Gorbunov, R. Rymzhanov, A. Volkov, Dependence of track etching kinetics on chemical reactivity around the ion path, Sci. Rep. 9 (2019) 15325. https://doi.org/10.1038/s41598-019-51748-y.

[14] P. Horn, M. Maurette, W. Von Oertzen, A study of the registration of arsenic and iodine ions in olivine and hypersthene crystals, Z. Naturforsch. A 22 (1967) 1793–1798. https://doi.org/10.1515/zna-1967-1117.

[15] V. K. Egorov, L. L. Kashkarov, N. G. Polukhina, V. A. Tsarev, On some structural features of olivine crystals from the Marjalahti meteorite, in: Proc. of the International Mineralogical Seminar “Structure and diversity of mineral world”, Syktyvkar, Russian Federation, June 17–19, 2008, Geoprint Institute of Geology, Komi Scientific Research Center, Ural Branch of the Russian Academy of Sciences, Russian Federation, 2008, pp. 139–140 (in Russian).

[16] A. V. Bagulya et al., Charge spectrum of superheavy nuclei of Galactic cosmic rays obtained in the OLIMPIYA experiment, Bull. Lebedev Phys. Inst. 42 (2015) 152–156. https://doi.org/10.3103/S1068335615050073.

[17] K. Lodders, H. Palme, H.-P. Gail, Abundances of the elements in the Solar System, in: Astronomy and Astrophysics, Landolt-Bornstein, New Series, Vol. VI/4B, Chap. 4.4, Ed. J. E. Trümper, Springer-Verlag, Berlin, Germany, 2009, pp. 560–630. https://doi.org/10.1007/978-3-540-88055-4_34.

[18] A. B. Aleksandrov et al., Simulation of passage of Galactic cosmic ray nuclei in meteorite–pallasite substance, Bull. Lebedev Phys. Inst. 40 (2013) 126–131. https://doi.org/10.3103/S1068335613050059.

[19] M. Maurette, P. Pellas, R. M. Walker, Cosmic-ray-induced particle tracks in a meteorite, Nature 204 (1964) 821–823. https://doi.org/10.1038/204821a0.

[20] O. Otgonsuren, V. P. Perelygin, S. G. Stetsenko, N. N. Gavrilova, C. Fieni, P. Pellas, Abundances of $Z > 52$ nuclei in Galactic cosmic rays: Long-term averages based on studies of pallasites, Astrophys. J. 210 (1976) 258–266. https://doi.org/10.1086/154826.

[21] V. P. Perelygin, Yu. V. Bondar, R. Brandt, W. Ensinger, R. L. Fleischer, L. I. Kravets, M. Rebetez, R. Spohr, P. Vater, S. G. Stetsenko, On search and identification of relatively short-lived superheavy nuclei ($Z \geqslant 110$) by fossil track studies of meteoritic and lunar olivine crystals, Phys. Atom. Nucl. 66 (2003) 1569–1573. https://doi.org/10.1134/1.1601767.

[22] A. Alexandrov, N. Konovalova, N. Okateva, N. Polukhina, N. Starkov, T. Shchedrina, Upgrade and new applications of the automated high-tech scanning facility PAVICOM for data processing of track detectors, Measurement 187 (2022) 110244. https://doi.org/10.1016/j.measurement.2021.110244.

[23] R. L. Fleischer, P. B. Price, R. M. Walker, Nuclear tracks in solids, California Press, Berkeley, 1973.

[24] A. B. Aleksandrov et al., Calibration measurements of the characteristics of tracks from superheavy nuclei in olivine crystals from meteorites, Instrum. Exp. Tech. 52 (2009) 187–190. https://doi.org/10.1134/S0020441209020079.

[25] N. Medvedev, A. E. Volkov, R. Rymzhanov, F. Akhmetov, S. Gorbunov, R. Voronkov, P. Babaev, Frontiers, challenges, and solutions in modeling of swift heavy ion effects in materials, J. Appl. Phys. 133 (2023) 100701. https://doi.org/10.1063/5.0128774.

[26] A. Alexandrov et al., History of heavy r-process elements in Galactic cosmic rays from nuclei tracks in meteorite olivine, Adv. Space Res. 70 (2022) 2674–2684. https://doi.org/10.1016/j.asr.2022.06.055.

[27] J. A. Johnson, Populating the periodic table: Nucleosynthesis of the elements, Science 363 (2019) 474–478. https://doi.org/10.1126/science.aau9540.

[28] D. L. Burris, C. A. Pilachowski, T. E. Armandroff, C. Sneden, J. J. Cowan, H. Roe, Neutron-capture elements in the Early Galaxy: Insights from a large sample of metal-poor giants, Astrophys. J. 544 (2000) 302–319. https://doi.org/10.1086/317172.

[29] N. Gehrels, Confidence limits for small numbers of events in astrophysical data, Astrophys. J. 303 (1986) 336–346. https://doi.org/10.1086/164079.

[30] V. Alexeev et al., Charge spectrum of heavy and superheavy components of Galactic cosmic rays: Results of the OLIMPIYA experiment, Astrophys. J. 829 (2016) 120. https://doi.org/10.3847/0004-637X/829/2/120.

[31] Yu. Ts. Oganessian, A. Sobiczewski, G. M. Ter-Akopian, Superheavy nuclei: From predictions to discovery, Phys. Scr. 92 (2017) 023003. https://doi.org/10.1088/1402-4896/aa53c1.

[32] Yu. Ts. Oganessian, V. K. Utyonkov, Super-heavy element research, Rep. Prog. Phys. 78 (2015) 036301. https://doi.org/10.1088/0034-4885/78/3/036301.

[33] I. Zvára, The Inorganic radiochemistry of heavy elements: Methods for studying gaseous compounds, Springer Dordrecht, Netherlands, 2008. https://doi.org/10.1007/978-1-4020-6602-3.

[34] B. L. Zhuikov, Methods of separation of volatile elements and oxides in the search for superheavy elements and in the production of radioisotopes, Synopsis of PhD Thesis, Moscow University Press, Moscow, Russian Federation, 1982 (in Russian).

[35] R. Eichler et al., Chemical characterization of element 112, Nature 447 (2007) 72–75. https://doi.org/10.1038/nature05761.

[36] B. L. Zhuikov, Theoretical calculation of the deposition temperature in thermochromatography from the thermodynamic data, Radiochemistry 61 (2019) 541–553. https://doi.org/10.1134/S1066362219050059.

[37] P. Yu. Apel et al., Study of etching features of quartz glass irradiated with xenon ions, Bull. Lebedev Phys. Inst. 51 (2024) 117–123. https://doi.org/10.3103/S1068335624600062.

[38] E. Andreev et al., Thermal properties of glass detectors for heavy ion registration, Techn. Phys. 70 (2025) 174–182. https://doi.org/10.61011/TP.2025.01.60524.272-24.

[39] E. V. Andreev et al., Testing natural and synthetic micas as detectors of accelerated heavy ions, Techn. Phys. 71 (2026) 180–190. https://doi.org/10.61011/TP.2026.01.62856.106-25.

[40] J. F. Ziegler, SRIM-2003, Nucl. Instrum. Meth. Phys. Res. B 219–220 (2004) 1027–1036. https://doi.org/10.1016/j.nimb.2004.01.208.

[41] N. Agafonova et al., The detection of neutrino interactions in the emulsion/lead target of the OPERA experiment, JINST 4 (2009) P06020. https://doi.org/10.1088/1748-0221/4/06/P06020.

[42] D. Abbaneo et al., Results and perspectives from the first two years of neutrino physics at the LHC by the SND@LHC experiment, Symmetry (Switzerland) 16 (2024) 702. https://doi.org/10.3390/sym16060702.

[43] A. Alexandrov et al., Muography of geometrically complex cultural heritage sites: Challenges and solutions on the example of searching for hidden anomalies on the ancient monastery territory in the Vologda Region, Phys. At. Nucl. 88 (2025) 616–632. https://doi.org/10.1134/s106377882570053x.